Overview of Radar-Based Gait Parameter Estimation Techniques for Fall Risk Assessment

Sevgi Z. Gurbuz, *Senior Member, IEEE*, Mohammad Mahbubur Rahman, *Member, IEEE*, Zahra Bassiri, and Dario Martelli

***Abstract*—Current methods for fall risk assessment rely on Quantitative Gait Analysis (QGA) using costly optical tracking systems, which are often only available at specialized laboratories that may not be easily accessible to rural communities. Radar placed in a home or assisted living facility can acquire continuous ambulatory recordings over extended durations of a subject's natural gait and activity. Thus, radar-based QGA has the potential to capture day-to-day variations in gait, is time efficient and removes the burden for the subject to come to a clinic, providing a more realistic picture of older adults' mobility. Although there has been research on gait-related health monitoring, most of this work focuses on classification-based methods, while only a few consider gait parameter estimation. On the one hand, metrics that are accurately and easily computable from radar data have not been demonstrated to have an established correlation with fall risk or other medical conditions; on the other hand, the accuracy of radar-based estimates of gait parameters that are well-accepted by the medical community as indicators of fall risk have not been adequately validated. This paper provides an overview of emerging radar-based techniques for gait parameter estimation, especially with emphasis on those relevant to fall risk. A pilot study that compares the accuracy of estimating gait parameters from different radar data representations – in particular, the micro-Doppler signature and skeletal point estimates – is conducted based on validation against an 8-camera, marker-based optical tracking system. The results of pilot study are discussed to assess the current state-of-the-art in radar-based QGA and potential directions for future research that can improve radar-based gait parameter estimation accuracy.**

***Index Terms*—Fall risk assessment, gait parameter estimation, micro-doppler, radar, skeleton estimation.**

***Impact Statement*— Quantitative Gait Analysis (QGA) relies on expensive optical tracking systems in specialized laboratories, whereas radar-based in-home QGA can capture daily gait variations, providing more realistic, continuous assessment of mobility.**

I. Introduction

HUMAN gait is an important health indicator, especially for older adults, who may increasingly experience issues with balance and stability as a normal part of the aging process. Monitoring of gait can provide early warning of diseases or important information on post-treatment recovery. As such, gait parameter estimation is an important task for any remote health monitoring system installed either in-home or in an assisted living facility in support of aging-in-place. Falls especially remain a significant threat to the health of older adults: according to the U.S. Center for Disease Control, each year, roughly 1,800 older adults suffer fall-related fatalities in assisted living facilities [1]. Thus, fall prevention and fall risk assessments are critical to preventing debilitating injury and fall-related fatalities.

Falls often occur during walking [2], [3], [4], [5] and although fall risk is influenced by a variety of intrinsic and extrinsic factors [6], gait and balance disorders have been consistently identified as one of the strongest risk factors. Not surprisingly, many studies suggest that gait features are associated with a history of falls and are good predictors of prospective falls [7]. Consequently, standardized gait assessments are commonly used in the clinical practice guidelines to evaluate and prevent fall risk [8], [9], [10], [11]. Numerous approaches have been taken to quantify gait and its relation to falls. Clinical rating scales usually integrate a cumulative score based on performance across multiple tasks. Accordingly, they are useful in evaluating mobility limitations and fall risk, but do not identify the specific mechanics that are associated with falls. Moreover, they may lack of discriminant ability, especially in healthy populations that have not started to fall frequently [12].

Quantitative gait analysis (QGA) may not only provide an indication of an individual's risk of falling, but also highlight specific modifiable gait characteristics that can be targeted with interventions to reduce the risk of future falls. Gait assessment

Manuscript received 28 February 2024; revised 9 April 2024 and 27 May 2024; accepted 27 May 2024. Date of publication 3 June 2024; date of current version 15 August 2024. This work was supported by the U.S. National Science Foundation under Grant 2238653 and Grant 2233503. The review of this article was arranged by Editor Bjoern Michael Eskofier. *(Corresponding author: Sevgi Z. Gurbuz.)*

Sevgi Z. Gurbuz is with the Department of Electrical and Computer Engineering, University of Alabama, Tuscaloosa, AL 35487 USA (e-mail: szgurbuz@ua.edu).

Mohammad Mahbubur Rahman is with the Advanced Radar Systems Team of Aptiv Corporation, Kokomo, IN 13085 USA.

Zahra Bassiri is with the Center for Motion Analysis in the Division of Orthopedic Surgery at Connecticut Children's, Farmington, CT 06032 USA.

Dario Martelli is with the Department of Orthopedics and Sports Medicine, MedStar Health Research Institute, Baltimore, MD 21218 USA.

Digital Object Identifier 10.1109/OJEMB.2024.3408078

can be altered to increase the level of difficulty (e.g., dual-task paradigms, turning, backward walking, and walking at a fast pace). Current methods for fall risk assessment with QGA rely on gait parameters extracted from optoelectronic motion capture systems, such as Vicon, which utilize markers on the participant to accurately estimate the position vs. time of each marker with multiple cameras. Such optical tracking systems are currently used in most gait analysis laboratories for both clinical and research purposes and provide a "gold standard" for gait analysis [13]. However, reliance on motion-capture based QGA systems involves expensive equipment, raising the cost of health care, while not being readily accessible as they are few, predominantly operated by medical schools in large cities, and thus distant from rural populations. These barriers can result in infrequent assessments and delays in diagnosis, especially for underserved or low-income adults. Moreover, QGA labs are controlled environments that preclude the assessment of natural gait: people invariably alter their behavior when they know they are being observed. This phenomenon is known as the Hawthorne effect and has been shown to influence gait [14]. For example, in the presence of an observer, limping was less pronounced and double support time more symmetrical in the gait of lower limb prosthesis users [15].

As a result, there has recently been great interest in the development of in-home QGA to enable continuous monitoring of gait in an uncontrolled environment, paving the way for reduced health care costs, more widespread access to gait assessments, and improved health outcomes. Both wearable and camera-based systems have been proposed for fall risk assessment [16], while radio frequency (RF) sensing – or radar – is a more recently proposed, emerging modality due to its ability to operate ambiently and in a non-contact fashion from a distance without requiring any light [17], [18]. This makes radar particularly well suited for monitoring in indoor settings, such as private homes and senior living communities, operating either in a stand-alone or complementary fashion with wearables, which may be forgotten to be worn, and cameras, which may not be preferred for ambient use as it may be intrusive of private moments and spaces. As such, radar can potentially offer continuous assessments even in sensitive settings without any burden on the user and operates ambiently without batteries. The RF emissions of typical radars are safe for humans, with levels at least 100 times less than that of a typical cell phone.

A radar placed in a home or assisted living facility can acquire continuous ambulatory recordings over extended durations of a subject's natural gait and activity. Radar-based QGA can capture day-to-day variations in gait, is time efficient and removes the burden for the subject to come to a clinic, providing a more realistic picture of older adults' mobility. This can aid in identifying psychological conditions, such as depression, which are marked by low activity levels, environmental factors that may be a cause of aberrations in gait, and early warning signs of neuromuscular disorders and potential fall risk – before a debilitating fall occurs.

Over the past decade, research on gait-related health monitoring with radar has focused on classification-based methods for fall detection [19], [20], [21], [22], gait/activity recognition [23], [24], [25], [26], [27], [28], [29], [30], [31], [32], [33], [34], aided/unaided ambulation discrimination [35], [36], [37], or detection of gait abnormalities [38], [39], [40], [41]. However, there have been fewer works that consider gait parameter estimation for QGA. On the one hand, many metrics that are accurately and easily computable from radar data have not yet been demonstrated to have an established correlation with fall risk or other medical conditions. On the other hand, the accuracy of estimated gait parameters that are well-accepted by the medical community as indicators of fall risk have not been adequately validated. Often, many works report the accuracy of the proposed radar-based estimation methods in comparison to the Kinect sensor or an assortment of web cameras; however, such markerless systems are more prone to significant estimation errors and thus offer inadequate assessment and benchmarking of true accuracy.

This paper provides an overview of emerging radar-based techniques for gait parameter estimation, especially with emphasis on those relevant to fall risk. The results of a pilot study comparing different radar-based estimation approaches are provided in conjunction with detailed discussion to provide comprehensive assessment of the current state-of-the-art and highlight areas requiring future research.

II. Radar-based Gait Parameter Estimation

The received signal of a typical frequency modulated continuous wave (FMCW) radar system for the backscatter from a point target is a time-shifted, frequency modulated version of the transmitted signal. Thus, the received backscatter, $s(t)$, from the entire human body can be represented as the superposition of reflections from each point on the surface of the body,

$$s\left(t\right) = \sum_{i=1}^{K} a_i e^{-j\left[2\pi f_0 t + \frac{4\pi}{\lambda} R_i(t)\right]} \tag{1}$$

where f_0 is the center transmit frequency, λ is the wavelength, t is time, $R_i(t)$ is the time-varying range of each point on the body to the radar transceiver, and a_i amplitude for the i^{th} point as computed from the radar range equation [42],

$$a_i = \frac{G\lambda\sqrt{P_i\sigma_i}}{\left(4\pi\right)^{3/2} R_i^2\left(t\right)\sqrt{L}} \tag{2}$$

Here G is the antenna gain, P_i is the transmitter power, σ_i, is the radar cross section (RCS) for each point target, and L represents losses, such as electronic noise.

Nowadays many commercially available radar systems also have multiple channels, or elements in their antenna array, so that the received multi-channel RF data stream can be reshaped into a 3D array: fast-time (number of analog-digital converter samples) $\times$ slow-time (number of pulses) $\times$ channel number. If the radar system has both a vertical and horizontal linear array, then the resulting RF data stream can be formed into a 4D array of fast-time, slow-time, vertical and horizontal channels.

Using radar signal processing, various 2D data representations may be computed [42], [43], [44]: micro-Doppler (μD) signatures, range-Doppler (RD) and range-Angle (RA) maps. RD maps are computed by taking a 2D Fast Fourier Transform (FFT) of the slow-time/fast-time data matrix for a single array

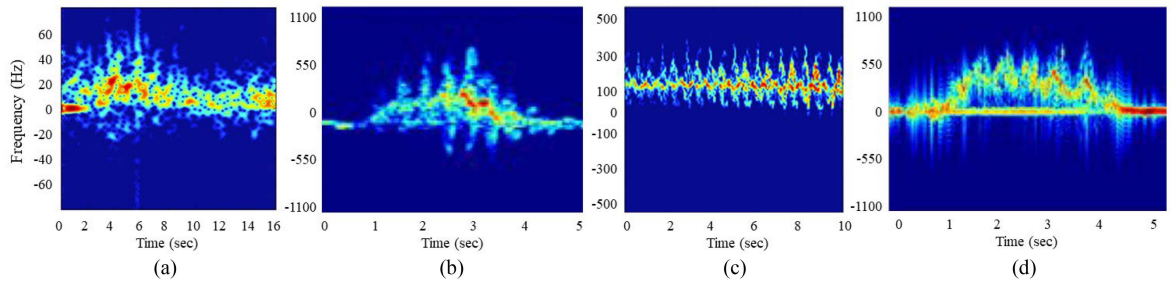

Fig. 1. Micro-Doppler signatures of a person walking as acquired from (a) 5.8 GHz pulsed doppler (PD) radar, (b) 10 GHz ultra-wide band impulse radar (UWB-IR), (c) 24 GHz continuous wave (CW) radar, and (d) 77 GHz FMCW radar with 4 GHz bandwidth.

element, while RA maps are found by computing the direction of arrival (angle) of the radar backscatter using methods such us the MUltiple Signal Classification (MUSIC) algorithm [45], [46]. Application of MUSIC for each coherent processing interval (CPI) during which N pulses are transmitted will result in a time-series of RA maps.

Most works on radar-based QGA derive the estimates from the radar μD signature [43], a representation of the velocity of the backscatter from each point of the body as a function of time. Micro-Doppler signatures are computed by applying a time-frequency transformation, such as the short-time Fourier Transform (STFT), across the slow-time samples of the radar data cube. To ensure that μD signatures are independent of the subject's range, cell averaging constant false alarm rate (CA-CFAR) detection [42] can be applied on RD maps to identify the range bins that include subject motion. Then, only these detected range bins are used in the computation of the μD signature.

The frequency, bandwidth and pulse repetition interval (PRI) of the transmitted signal can affect the accuracy of the gait parameter estimates derived from μD signatures. The depth resolution (Δr) of an FMCW radar reflects the ability of the radar to differentiate between the radial distance, or slant range, between two point scatterers and is computed as $\Delta r = c/2\beta$, where c is the speed of light and β is the transmitted signal bandwidth. The velocity resolution $\Delta v = \lambda/(N \cdot PRI)$, where N is the number of pulses transmitted over a CPI. Thus, the higher the transmit frequency of the radar, the shorter the wavelength, and the smaller the differences in velocity that can be resolved. Note that range and velocity resolution differ from the size of the range and velocity bins, which indicate size of each pixel. The size of a range bin is given by $r_b = (c/2)t_s$, where t_s is the sampling interval of the analog-to-digital converter of the radar. The size of a velocity bin is computed as $v_b = \lambda/(2 \cdot PRI \cdot N_{fft})$, where N_{fft} is the number of FFT points utilized. The angular resolution of a multi-channel radar depends on the beamwidth of the main lobe of the antenna beam pattern, and can be computed as $\theta = K\lambda/D$, where K is the beamwidth factor and D is the size of the aperture. Beamforming techniques [47] can be utilized to form larger virtual arrays and improve the angular resolution of a radar.

The impact of different radar transceiver parameters may be observed from the sample μD signatures shown in Fig. 1 for a person walking as acquired by four different radars: a 5.8 GHz pulsed doppler (PD) radar, 10 GHz ultra-wide band impulse radar (UWB-IR), 2.4 GHz continuous wave (CW) radar, and 77 GHz FMCW radar with 4 GHz bandwidth. The ground clutter returns, which result from backscatter from stationary objects/surfaces in the environment, result in a horizontal line at 0 Hz. This is most clearly observed in the 77 GHz μD signature shown in Fig. 1(d), where the oscillatory characteristics of the gait cycle in the human return can be clearly visually differentiated from the 0 Hz clutter line. These clutter returns can be filtered out using a Butterworth low pass filter or techniques such as Moving Target Indication (MTI) [42], as illustrated with the signatures of Fig. 1(a)–(c).

The torso response is often the body part that results in the strongest backscatter and may be identified as a reddish sinusoidal curve in the μD signature. At low frequencies, such as the 5.8 GHz, the periodicities of the gait cycle are not as clearly observed as in the higher frequencies. Moreover, the average velocity of the gait signature appears at lower Doppler shift frequencies when the transmit frequency is lower. This increases the likelihood of the clutter returns masking the low frequency components of the gait signature – an effect that can degrade the accuracy of gait parameter estimates or gait classification algorithms. While millimeter wave frequency transmissions result in data with the most evident limb trajectories, higher frequencies also suffer from more significant atmospheric attenuation, as may be seen by the inverse relationship between the signal amplitude a_i and frequency (since $f = c/\lambda$) captured in (2).

The pulse repetition frequency (PRF), which is the inverse of the PRI, also determines the maximum Doppler shift that can be acquired by a radar unambiguously. If the PRF is lower than the Doppler shift incurred by the maximum speed of movement, aliasing occurs in which the high frequency parts of the signature will wrap around to the bottom of the image. Such effects are highly detrimental to gait analysis algorithms, which typically rely on capture of unaliased μD signatures.

Note that as the cost of a radar system often depends on the transmit frequency, bandwidth and number of antenna elements in azimuth and elevation, an important question that merits further investigation is what the minimum transmission requirements are to achieve a certain level of accuracy in gait parameter estimates for QGA in real-world conditions. The

radar transmission also affects the sample size in each of the dimensions of the radar data tensor; thus, the transmission parameters also influence computational complexity and may be a limiting factor in situations requiring real-time QGA.

A key limitation of μD-based gait parameter estimation is that the μD signatures represent the aggregate backscatter from the entire human body – not a specific body part or joint. This makes recent advancements in RF skeleton estimation interesting to consider from the perspective of QGA. However, most RF skeleton estimation methods utilize deep neural networks (DNNs) to learn a mapping between various types of radar representations to skeletal key points. Thus, the methods are very data greedy and have been primarily considered in the broad context of monitoring activities of daily living – a task that does not require the same level of estimation accuracy as gait parameter estimation for QGA. The pilot study presented in Section IV provides a gold standard comparison of estimation accuracy from both μD signatures and RF skeletons under a moderate amount of data. Relevant results from the literature are discussed next.

A. QGA Using RF Micro-Doppler Signatures

Early works on radar-based gait analysis [48], [49] focused on the estimation of walking speed by averaging the speed corresponding the strongest (peak) return in the μD signature, which typically results from torso backscatter. Later, when it was shown that backscatter from a person could be well approximated by (1) utilizing superposition [50], [51], biomechanical models – such as the Boulic walking model [52], which provided parametric equations and graphs representing body part trajectories and joint angles – were exploited to estimate the height and speed of a person walking [53], [54].

While early works did not involve gold standard comparisons, in 2014, a study [55] was conducted that investigated the estimation accuracy of walking speed and step time, comparing the estimation accuracy attained over a 17-ft walkway using a 5.8 GHz foot-level and torso-level radar with that of a Vicon-based optical tracking system. Excellent agreement between radar and Vicon-based estimates were found for step time estimation using the foot-level radar; however, for walking speed, the impact of aspect angle on velocity-estimates was noted as a cause for an offset between radar and Vicon-based estimates. This offset was less in the torso-level radar data and more pronounced in the foot-level radar data. This result is not surprising, considering that the Doppler shift is proportional to radial velocity, not absolute velocity.

To mitigate the impact of aspect angle in QGA methods based solely on μD signatures, researchers have proposed utilizing radar systems for gait analysis in hallways, which would preclude significant angular deviation from the radar line of sight. For example, in [56], walking speed, step points, step time, step length, and step count are estimated from a radar monitoring a 14 m. hallway. Alternatively, [57] has proposed utilizing radar for walking tests administered by physical therapists, whereby the subject would walk along a straight path away from the radar, turn around, and then walk back towards the radar. Analysis of radar μD signatures was utilized to segment the data into three segments: an acceleration zone, a measured-gait zone, and a deceleration zone. The resulting gait speed estimate was validated against a Vicon motion capture system and found to have an error of 0.076 m/s.

More advanced signal processing techniques have also been proposed to track limb motion during ambulation and enable angle-agnostic μD-based QGA. In [58], a 1-D block processing method is proposed to use CW radar to track the arm, elbow, hand, torso, knees, calf or ankle under various types of walking – walking without hands moving and walking with one arm or both arms swinging. The maximum speed of tracked body parts is reported in comparison with that obtained using the Boulic model. While the method appeared effective in extracting lower limb motion during ambulation, tracking the hand and arm movements was less reliable. Aside from CW radar, researchers have also proposed using Stepped-Frequency CW (SFCW) radar with a rapid pulse repetition frequency (PRF) to track fast motions of various parts of the body [59].

Despite the limitations of angular dependence, μD-based QGA has been shown to have great potential in extracting a much broader range of gait parameters than just gait speed. In [60], an ultrawide-band impulse radar (IR-UWB) was used to estimate not just walking speed, but also step length, cadence, stride length, step frequency, lower limb orientation, and total traversed distance. The IR-UWB radar estimates were seen to correspond well with estimates obtained from the accelerometer and gyroscopic sensors on a smartphone. Using the peak of the μD signature as reflective of the trunk velocity profile, [61] compared the estimation accuracy of stride time, step time, step length, swing time and stance time for a 24 GHz CW radar and Vicon systems. A comparison of the impact of having a single versus multi-channel FMCW radar system on an analysis of gait variability is given in [62], while also showing the assessment accuracy in comparison with Vicon data. This work was extended in [63] to consider step time variability via radar data acquired over continuous streams of activity data collected in an unconstrained environment. The continuous data is segmented and sequentially classified to extract the intervals over which the subjects are walking. The impact of segmentation accuracy on step time variability is discussed.

While these aforementioned works focused on estimation based on the trunk profile, other works have proposed the estimation of gait parameters from the envelopes of the μD signatures. The envelopes represent the speed of maximum (forward or backward) movement on the body, which is typically caused by the movement of the feet. Thus, without explicitly tracking the feet, several researchers [64] have estimated a broader range of gait parameters by extracting envelopes of the toe, ankle and knee from the μD signature: stride time, stance time, flight time, step time, cadence, stride length, step length, maximal foot velocity, maximal ankle velocity, maximal knee velocity, and time instant of maximal knee velocity. Based on comparisons against a 3D motion capture system with 12 infrared cameras, radar-based estimates were found to match well for most of the gait parameters extracted. Furthermore, it was proposed that

symmetry (or asymmetry) in the micro-Doppler signature could be characterized as an indicator of gait abnormality [39].

Similarly, simulation-based studies [65], [66] have proposed extraction of twelve different gait metrics from the torso profile and envelopes of the μD signature, including 1) mean body velocity (gait speed), 2) degree of variation in body velocities, 3) maximum body velocity, 4) minimum body velocity, 5) mean leg velocity in swing phase, 6) degree of variation of leg velocities in swing phase, 7) maximum leg velocity, 8) minimum leg velocity in swing phase, 9) mean leg velocity in stance phase, 10) degree of variation of leg velocity in stance phase, 11) maximum leg velocity in stance phase, and 12) minimum leg velocity. These metrics were then utilized to categorize participants as fallers or non-fallers.

Subsequently, a study [67], [68], [69] experimentally validating these simulation results was conducted by recruiting older adults aged 65 and above, who are able to walk without assistance of another person or walking aide, from a senior day care center and rural community center. The participants were given a questionnaire about their fall history within the past year, based upon which they were divided into one group of non-fallers (19 people, mean age 78.8) and fallers (14 people, mean age 82.5). Participants were then asked to walk for 10 meters, during which time their gait was measured using a micro-Doppler radar. Four gait parameters (1, 5, 6, 10) were extracted from the micro-Doppler signatures and used to classify participants as fallers or non-fallers with an accuracy of 78.8%. In another study [68], [69] involving 74 older adults aged 75 years and above, a subset of these radar-based gait parameters (1, 5, 6, 7, 9, and 10) were also shown to correlate well with the results of four cognitive function tests – the Mini Mental State Examination (MMSE), Digit Symbol Substitution Test (DSST), Scenery Picture Memory Test (SPMT), and Verbal Fluency Test (VFT) – and were used to classify participants according to high / low cognitive function.

More recently, automation of the Timed Up and Go (TUG) test, which is an established, standardized test used in clinical practice for assessing mobility and fall risk, has been proposed using radar. In [70], an ultra-wide band (UWB) radar was utilized to segment and estimate the stride length during execution of a TUG test, comparing the accuracy of radar estimates against those acquired from sensors placed in the insole of a shoe. This study found that the risk scores obtained using an insole containing three force sensors and y-axis of acceleration were comparable to that attained using a single radar and two force sensors. In another study [71], also using UWB, measurements of walking duration, turning duration, and gait speed acquired during a TUG test were shown to correlate well to measurements acquired from a video-based system.

In 2023, the first radar-based system to fully automate the TUG test measurements was proposed [72] in which data from a CW Doppler radar was processed to segment the continuous data steam according to "transfer" and "walk" phases as well as "walk" and "turn" phases. Afterwards, gait parameters, such as the number of steps, step time, gait cycle duration, swing time, average walking speed, cadence, TUG walking speed duration, TUG duration, step time, and stride length were computed from the radar micro-Doppler signature. The study was conducted on 26 healthy subjects, aged between 22 and 60, who performed three TUG trials at slow, normal and fast speed, leading to a total of 9 trials per subject. Data was acquired simultaneously from the CW radar and a Vicon motion capture system to validate radar-based measurements. High correlation coefficients were obtained for the torso speed, limb oscillations, initial and final indices of the TUG phases and extracted gait parameters. As such, this work represents the first to show experimental results indicating the feasibility of automating TUG tests using radar.

B. QGA Using Joint RF Data Representations

Although μD-based QGA has the benefit of being applicable to any kind of radar, including the lowest-cost, least complex CW radars, the limitations brough by aspect angle dependency and the increasing availability of multi-channel RF transceivers at lower and lower costs has driven research into QGA based on joint RF domain representations, such as the radar data cube, which captures not just velocity information, but also information about range and angle as a function of time. Techniques such as multi-dimensional principal component analysis (PCA) have been proposed for exploiting the radar data cube for activity recognition [73] and fall detection [74]. In [75], a joint domain multi-input, multi-task learning (JD-MIMTL) network is proposed that takes not just stacked snapshots of μD, but also range-Doppler and range-Angle maps as input to identify when a person is walking and subsequently extract the torso velocity and acceleration to assess gait variability.

In [76], a FMCW radar is used to track subjects [77] as they move freely in the home, extracting the stable phase of walking intervals (which excludes acceleration and deceleration phases), so as to monitor the gait speed of 50 participants, with and without Parkinson's disease, for up to a year. The study showed that at-home gait speed, as estimated using radar, strongly correlates with gold-standard assessments of Parkinson's disease, such as the Movement Disorder Society-Sponsored Revision of the Unified Parkinson's Disease Rating Scale (MDS-UPDRS) part III sub-score and total score.

Beyond just estimation of gait speed and torso profile, several studies have also exploited the range, angle and velocity information of the radar to improve limb tracking. For example, [78] separately recognized the legs in the range-Doppler map and extracted the range and velocity profile for each leg. Using these profiles, stride time, stance time, flight time, step time, cadence, maximum foot velocity and its interval were estimated. A new metric, the Gait Asymmetry Indicator (GAI), computed as

$$GAI = \left| \frac{MFV_R}{MFV_L} - 1 \right| \tag{3}$$

where MFV_L and MFV_R represents the maximum foot velocity of the left (L) and right (R) legs, respectively, was proposed to detect gait abnormality. The results were validated through comparison with Inertial Measurement Unit (IMU) data over 15 participants in 4 scenarios (walking, running, left leg limping, and right leg limping) using the intraclass correlation value, which showed good agreement except for flight time.

Another study [79] utilizing synthetic range-Doppler versus time data simulated from a skeletal model proposes trajectory tracking using Kalman filtering and weighted joint nearest neighbor algorithm for data association. Trajectory tracking accuracies ranging of as much as 99.6% is reported, while the estimates of kinematic gait features – such as step length, stride speed, stride frequency, gait phase, step length symmetry, phase symmetry, acceleration time constant of forearms, and skewness of thighs – are reported to have 91.9%–93.8% accuracy. While limb tracking techniques show promise, the accuracy of current methods on real radar data has not yet been adequately evaluated. Advancement of more effective methods for limb tracking remains an open area of research.

C. QGA Using RF Skeletons

The task of tracking limbs through micro-Doppler data encounters obstacles due to human motion's intricate and dynamic properties, where distinguishing between overlapping signals and the slight movements of minor limbs poses accuracy challenges. Yet, the potential of leveraging high-dimensional RF data (spanning range, angle, and Doppler) for radar-based pose estimation in limb motion tracking is promising. Progress in signal processing and machine learning, particularly with the integration of Convolutional Neural Networks (CNNs), enhances accuracy and the capacity to detect minor movements, bringing non-invasive, real-time limb tracking closer to reality.

Initially explored with the proposal of RF-Capture [80] in 2015, radar-based human skeleton estimation utilizes 5.4 to 7.2 GHz FMCW signals via an antenna array to detect coarse body part positions, subsequently reconstructing a human figure by piecing together these detected parts. In 2018, RF-Pose3D [81] advanced this framework by employing a T-shaped 12-element antenna array for FMCW signal transmission and reception at a 6.3 GHz center frequency and 1.8 GHz bandwidth. This system feeds range-azimuth and range-elevation heatmaps into a Resnet-based encoder neural network, coupled with 12 camera nodes capturing RGB video to collect label key points from OpenPose for training a region proposal network (RPN) and a ResNet-architecture CNN. This network focuses on RF data from individual persons to extract 3D skeletons from regions of interest, reporting average localization errors of 4.2, 4.0, and 4.9 cm in the x, y, z axes, respectively, with OpenPose estimated key points. Despite its groundbreaking demonstration of RF skeleton estimation's feasibility, the method's reliance on over 17 million data samples and 16 hours of recordings underscored its significant data and computational demands, limiting practical application.

In 2020, mmPose [82] was proposed, which predicted more than 15 joints using two specially oriented IWR1443 radars. This method, feeding point clouds into a bifurcated CNN, did not utilize the radar's Doppler and signal intensity data, leading to jitter in skeleton animation. Attempts in 2022 with additional filters [83] sought to reduce jitter for a more stable skeleton representation but did not fundamentally enhance accuracy. In 2021, another approach, MARS [84], was proposed, which employed IWR1443 radar and standard software for point cloud data, including Doppler and intensity information, reporting average MAE of 5.8cm accuracies in 19-point predictions compared to Microsoft Kinect v2 camera estimates. They further investigated joint angle estimation from the predicted skeleton and reported the average MAE of MARS in estimating left elbow angle, right elbow angle, left knee angle, and right knee angles are 12°, 13°, 7°, and 6°, respectively.

In recent years, there has been a significant surge in publications focused on mm-wave-based human pose estimation [85], [86], [87], [88], [89], [90], [91], [92], [93]. Generally, these studies employ radar-generated range-azimuth and range-elevation heatmaps, with some also incorporating radar point clouds, as data inputs for training their deep neural network (DNN) models. For validating their findings, the bulk of these studies have predominantly leaned on either the Kinect system or the multi-camera-based OpenPose model for ground truth. This approach presents substantial challenges in the realm of RF skeleton estimation. On one hand, the Kinect system, when employed as a benchmark for ground truth, is problematic due to its considerable errors in skeleton tracking. One study [94] showed that Kinect tends to provide an oversimplified version of the actual skeleton, with its estimates often deviating from those obtained through marker-based tracking methods. On the other hand, systems employing multiple cameras, such as OpenPose, introduce their own complexities. While Kinect's limitations stem from its inherent technology, the use of OpenPose, which relies on a multi-camera setup, is cumbersome and less practical for deployment. Furthermore, reliance on OpenPose has been shown [95] to introduce specific inaccuracies, including consistent biases in the estimation of knee and ankle joints, and relative biases in trunk and hip joints, in comparison to the estimations derived from optoelectronics motion capture systems, a more precise skeletal tracking method.

Hence, current QGA using RF skeleton has been limited to only estimating the skeleton coordinates. These efforts are constrained by key challenges, including the poor elevation angular resolution of the available off-the-shelf RF sensors, inappropriate use of Kinect for ground truth due to significant estimation errors, the impracticality of bulky multi-camera systems, and inaccuracies introduced by relying on the OpenPose model. Moreover, the dependency on complex, data-intensive models necessitates the exploration of more efficient models requiring less data, crucial for enabling practical skeletal estimation on mobile computing platforms.

III. Pilot Study

To evaluate and compare different radar-based QGA techniques, a pilot study was conducted in which both radar and motion capture data were simultaneously acquired from participants who walked back and forth in an indoor lab at the University of Alabama.

A. Experimental Design and Data Collection

Five healthy, right-foot males (25.6 $\pm$ 1.9 years, 70.6 $\pm$ 17.5 kg, 1.75 $\pm$ 0.093 m) completed the experiment. All participants i) had no known history of neurological or musculoskeletal

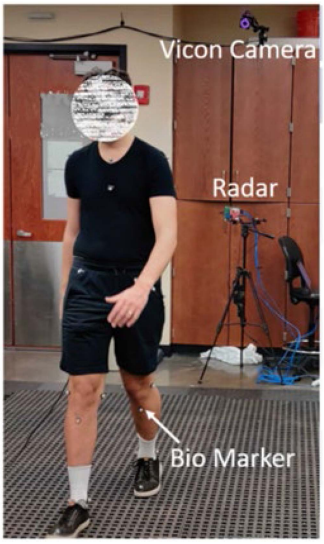

Fig. 2. Experimental setup during data acquisition.

disorders; ii) were naïve to the experimental conditions; iii) had a normal or corrected-to-normal vision. Study procedures were approved by the Institutional Review Board at the University of Alabama under Protocols #18-06-1271, #21-10-5055 and #23-04-6553.

The RF data were acquired using a Texas Instruments (TI) IWR2243 Cascade radar, operating in the 77 GHz–81 GHz frequency band with 12 Tx and 16 Rx antennas, positioned at the start of the walkway at about 1 meter height and aligned with the direction of walking, as shown in Fig. 2. The TI radar was configured to utilize Time Division Multiplexing (TDM) to create 192 virtual Multi-Input Multi-Output (MIMO) channels. Out of these, 58 elements overlap in the azimuth plane, leaving only 86 non-overlapping channels designated for azimuth virtual antennas. Regarding the elevation, there are 7 elevation planes comprise an aperture size of 6 $\lambda/2$. However, within this aperture, 3 planes are empty, and only 4 active elements/channels are allocated for elevation measurements. Additionally, there are 44 redundant elements in the elevation that do not comprise aperture larger than 6 $\lambda/2$, therefore remain unused. Here λ is the wavelength of the transmitted signal. Fig. 3 illustrates the virtual antenna array for this radar. Each radar chirp was comprised of 256 analog-to-digital converter (ADC) samples, with a total of 128 chirp-loops per frame being transmitted. Consequently, the raw ADC data was organized into range-azimuth (256x86), range-elevation (256x7), and range-Doppler (256x128) planes.

Participants walked for five minutes at self-selected speed up and down a 6-meter walkway. A total of 41 reflective markers (MRKs) were attached to the whole body to record 3-D position data with an 8-camera motion capture system at a sample frequency of 100 Hz (NEXUS software and VERO infra-red Cameras, Vicon Motion Systems). To establish basic synchronization between the two recording systems, we initiated recordings simultaneously with a voice command while participants performed a fast "air punching" movement, clearly detected by both systems. Subsequently, we identified the radar frame displaying this rapid movement from the radar range-Doppler maps. Similarly, we pinpointed the frame in the Vicon skeleton data showing the hand punching forward. By aligning these two frames, we synchronized the two systems. Given that the radar operates at 10 Hz and Vicon operates at 100 Hz, we down sampled the Vicon frame to match the radar frame rate, ensuring we have a ground truth Vicon frame for each radar frame.

B. RF Skeleton Estimation Under Limited Data

In this work, we consider RF skeleton estimation when a limited amount of data is available for training. To quantify the estimation uncertainty due to the trained deep neural network (DNN) utilized for skeleton estimation versus other sources of estimation error, such as the resolution of the RF sensor or real-world effects, such as multipath reflections, we compare the skeleton estimation accuracy obtained when using simulated (SkelS) versus real (SkelR) RF data. In particular, we synthesize [96], [97], [98] the expected radar return using (1) and (2), where the time-varying ranges R_i to the i^{th} point are derived from the concurrently acquired Vicon motion capture measurements. When generating the simulated data, we deliberately restricted ourselves to using only 20 azimuth antenna elements/planes instead of the full 86 elements found in the real radar. This choice was made because the azimuth angular resolution in the real data is already quite high, enabling the deep neural network (DNN) model to effectively learn from it. Consequently, we reduced the number of azimuth antenna elements in the simulation to avoid generating an overwhelming amount of data. Conversely, we used 7 elevation planes with a 6 $\lambda/2$ aperture, ensuring no empty elements. This provides finer angular resolution in elevation compared to the real data's 4 elevation channels. Pre-training with this higher-resolution data helps set DNN weights at favorable local minima, improving feature representation learning during fine-tuning with coarse-resolution real data.

To reduce the dimensionality of both the measured and simulated RF data so that the resulting DNN for skeleton estimation is less complex and requires less data for training, we developed a 'max per range bin' and 'max per angle bin' method to capture the main features from the RF heatmaps. As the name suggests, this process finds the maximum intensity value at each range/angle bin to capture the variations of the return signal's strength over range and angle bins. This approach offers several benefits: first, it enables the representation of a 2D heatmap with just two vectors. For example, a 256x256 range-azimuth heatmap can be condensed into a 256x2 size array. Here, one vector represents the maximum per range bin (256x1), and the other captures the maximum per azimuth angle bin (256x1), markedly simplifying the challenge of managing extensive data matrices in DNNs. Consequently, for a set comprising both range-azimuth and range-elevation heatmaps, the result is a compact array sized 256x4. Second, this approach accurately maintains the gross velocity information by correctly capturing the movement of the target's peaks from one frame to the next. Third, as the dimensionality of the data is reduced, it enables a simpler neural network to effectively extract the necessary information for determining range, azimuth, and elevation. Thus, after

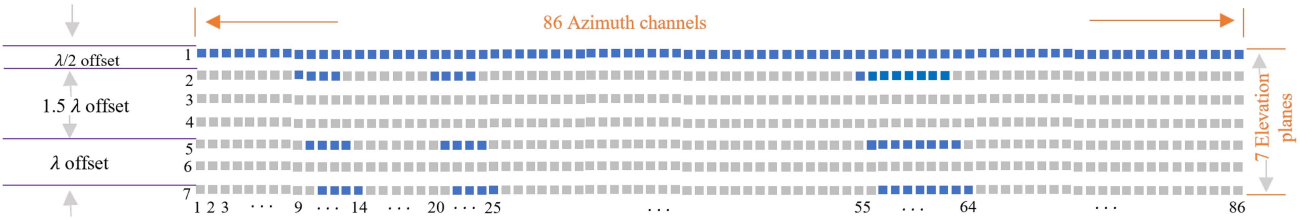

Fig. 3. Virtual antena array for TI AWR 2243 cascade radar.

aggregating all frames, the data's total size becomes 27,408 x256x4. This is subsequently reshaped to 2,284x12x256x4 to incorporate the time dimension, the size of which was determined through empirical methods.

Next, a lightweight 3D CNN + Long Short-Term Memory (LSTM) model is designed to capture both the temporal and spatial characteristics for predicting the 3D coordinates of 14 skeleton joints. The architecture is comprised of a 3D convolutional layer, followed by batch normalization, max pooling, dropout, and two bi-directional LSTM layers. It culminates in a time-distributed dense layer equipped with 42 neurons (reflecting 14 joints times 3 coordinates per joint) and employs a linear activation function.

The Huber loss function [99]

$$L\delta\ (\mathrm{y}, \mathrm{f}\,(\mathrm{x})) = \begin{cases} \frac{1}{2}(y - f\,(x))^2, & for\ |y - f\,(x)| \leq \delta, \\ \delta\,|y - f\,(x)| - \frac{\delta^2}{2}, & otherwise \end{cases} \quad (4)$$

is utilized for model optimization. It offers robust regression by being less affected by data outliers compared to the squared error loss. The Huber loss switches between Mean Squared Error (MSE) for small prediction errors and Mean Absolute Error (MAE) for large prediction errors, with the switch occurring at a specified threshold, delta (δ). When the prediction error is within the delta range, it utilizes MSE, which penalizes small errors more heavily and aids in fine-tuning the model's predictions. If the error exceeds delta, indicating a potentially large or outlier error, it uses MAE, which treats all errors linearly, thereby reducing the impact of outliers. This creates a more robust model by combining the sensitivity of MSE to small errors with the outlier resistance of MAE for large errors. For this key point regression model, δ=1 was used.

Among other hyperparameters, a learning rate of 0.0021, batch size of 32, and the model was trained for 80 epochs. The training was conducted using a leave-one-out approach, which was applied across the data from all subjects. On average, each subject's data consisted of approximately 5,600 pairs of radar frames. For every frame, the model was designed to predict 42 key points.

Initially, the model was trained and tested with simulated data with a leave-one-subject-out method, resulting in Mean Absolute Errors (MAE) of 3.15 cm for the medio-lateral (ML) axis, 4.37 cm for the vertical (V) axis, and 1.4 cm for the antero-posterior (AP) axis. Subsequently, when this model pre-trained using simulated data was further refined (fine-tuned) using measured radar data, the MAEs increased to 5.63 cm for the ML axis, 7.30 cm for the V axis, and 7.81 cm for the AP axis. After predicting the RF based skeleton trajectories for all subjects, we increased its sampling rate to 100 Hz using linear interpolation. This adjustment was made to align the RF based skeleton trajectories with the original frame rate of the Vicon system, which operates at 100 Hz. It's worth noting that interpolation wasn't necessary for the Vicon data itself, given its native sampling rate of 100 Hz.

Fig. 4(a) illustrates the 3D trajectories of the midpoint between the hips, left ankle, and right ankle extrapolated from the simulated radar data (SkelS), the actual radar data (SkelR), and the motion capture data (MRK) during four laps of a representative subject's trial. Fig. 4(b) illustrates the reconstructed skeleton from the three measurement systems for a single time frame.

It's important to note that, for this application, minor misalignment between the RF and Vicon trajectories wasn't a significant concern. Our focus was primarily on gathering discrete gait parameters, such as step time and step length, by considering the time difference between corresponding points in each system.

C. Data Analysis for Gold Standard Comparison

High-frequency related noise was removed from position data estimated with markers' coordinates (MRK), RF skeleton from real data (SkelR), and RF skeleton from simulated data (SkelS) by low-pass filtering at 10 Hz (zero-lag, fourth-order Butterworth low-pass filter). For MRK, heel strikes were estimated by finding the farthest anterior position of the heels position relative to the sacrum. For SkelR and SkelS, heel strikes were estimated by finding the farthest anterior position of the ankles position relative to the mid-point of the hips. Step length was estimated as the absolute distance in the AP direction of the ankle markers from heel-strike to heel-strike.

The μD signature was computed as in our previous works [62], [63]. The trunk radial velocity (V_{RF}) was estimated by finding the peak μD signature intensity, which indicates the highest reflected energy. Indeed, it can be assumed that the strongest signal in the μD signature is due to the trunk motion, as the trunk comprises the largest radar cross-section of the body. High-frequency noise was removed by low-pass filtering V_{RF} data at 5 Hz [61]. Trunk acceleration was calculated as the first derivative of V_{RF} using a central finite difference method. Heel strikes were estimated by finding the zero-crossing points of the trunk acceleration curve, after low-pass filtering at 2 Hz [100]. The absolute value of V_{RF} was subdivided into steps. Step length was estimated as the area under the curve of V_{RF} over a step cycle.

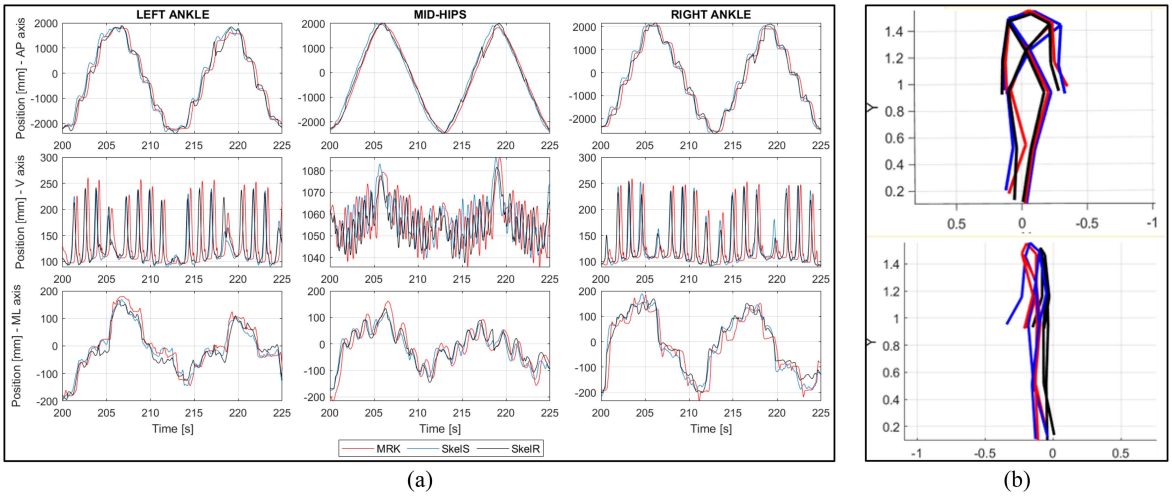

Fig. 4. (a) Representative trajectories of the left ankle, right ankle, and midpoint of the hips along the Antero-Posterior (AP), Medio-Lateral (ML), and Vertical (V) axes for the three measurement systems. (b) Frontal and sagittal views of the 3D skeleton reconstruction of the three measurement systems for a single time frame. Motion capture (MRK, red line), Skeleton from simulated radar data (SkelS, blue line), and Skeleton from real radar data (SkelR, black line).

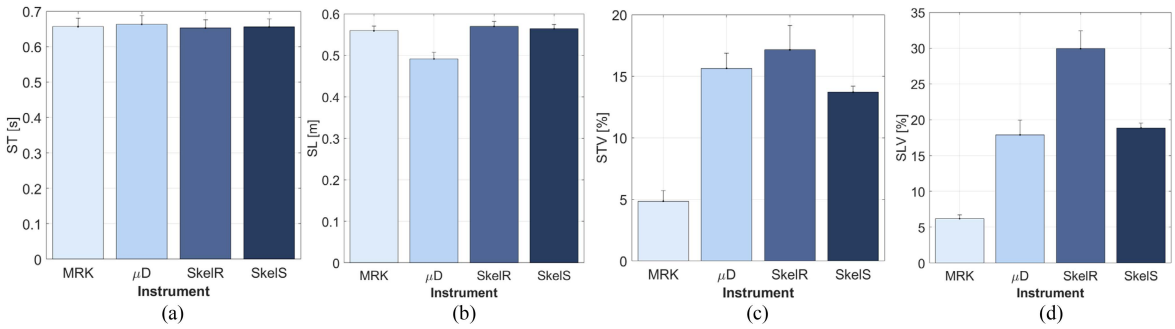

Fig. 5. (a) Stride Time (ST), (b) Step Length (SL), (c) ST Variability (STV), and (d) SL Variability (SLV) obtained for Markers (MRK), RF micro doppler (μD), RF skeleton from real data (SkelR), RF skeleton from simulated data (SkelS). Bars refer to the standard error.

For each run, the middle 5 steps were included in the analysis to ensure a steady walking state. For all methods, step time was computed as the time interval between consecutive heel strikes. Then, step time (ST), step length (SL), and their variabilities (STV, SLV) were defined as the mean and the coefficient of variation of all accounted steps over the five minutes of walking. The coefficient of variation was computed as the percentage of the ratio between standard deviation and mean value. Differences between the MRK method and the three types of RF methods were expressed as mean of the differences (MD), mean percent difference (MPD), and 95% ratio limits of agreement (LOA). LOA was calculated as 1.96 times the standard deviation of MPD. |MPD+LOA| values >50% were interpreted as poor, 10%–50% as moderate, 5%–10% as good, and < 5% as excellent agreement [101].

D. Results

Fig. 5 shows the mean and standard deviation of the outcome variables extracted from each measuring system (i.e., MRK, μD, SkelR, SkelS). Table I reports the summary metrics for the differences between the gait parameters extracted with MRK and each RF method.

Independently by the RF method used, ST showed excellent agreement (|MD|<0.007s; |MPD+LOA|<3.3%) with the μD method overestimating ST while both skeleton methods slightly underestimating ST. SL showed good agreement when estimated with the μD (|MD|=0.068m; |MPD+LOA|=8.9%), and excellent agreement when estimated with the SkelR and SkelS methods (|MD|<0.010m; |MPD+LOA|<2%). The μD method underestimated SL while both skeleton methods slightly overestimated SL. STV showed poor agreement when estimated with the μD and SkelS methods (|MD|<10.8%; |MPD+LOA|>52.0%) and moderate agreement when estimated with the SkelR method (MD=12.3%; |MPD+LOA|=17.8%) with values obtained with RF methods systematically larger than those obtained with the MRK method. Noticeably, SkelS showed the lowest absolute error (MD=8.85%) but resulted in poorer agreement due to a larger standard deviation. For all methods, SLV showed moderate agreement (|MD|<23.7%; |MPD+LOA|<37.6%),

TABLE I
CONCURRENT VALIDITY

Variable	MRK Vs. μD			MRK Vs. SkelR			MRK Vs. SkelS		
	MD (Mean ± STD)	MPD [%] (Mean ± SD)	LOA [%]	MD (Mean ± STD)	MPD [%] (Mean ± SD)	LOA [%]	MD (Mean ± STD)	MPD [%] (Mean ± SD)	LOA [%]
ST [s]	0.007 ± 0.011	1.00 ± 1.71	3.3	-0.004 ± 0.007	-0.54 ± 1.09	2.1	-0.001 ± 0.005	-0.12 ± 0.76	1.5
SL [m]	-0.068 ± 0.022	-13.03 ± 4.52	8.9	0.010 ± 0.006	1.84 ± 1.05	2.0	0.005 ± 0.004	0.90 ± 0.72	1.4
STV [%]	10.79 ± 3.87	105.65 ± 33.74	66.1	12.29 ± 2.57	113.59 ± 9.06	17.8	8.85 ± 1.77	97.95 ± 26.51	52.0
SLV [%]	11.70 ± 4.17	95.13 ± 19.17	37.6	23.74 ± 5.72	130.35 ± 16.53	32.4	12.65 ± 0.94	101.58 ± 9.49	18.6

Measurement method: Markers (MRK), RF micro doppler (μD), RF skeleton from real data (SkelR), RF skeleton from simulated data (SkelS).
Gait Parameters: Stride Time (ST), Step Length (SL), ST Variability (STV), and SL Variability (SLV).
Concurrent Validity: Mean difference (MD), mean percentage difference (MPD), and 95% ratio limits of agreement (LOA) between the gait parameters obtained with the MRK and the three RF methods. A positive sign indicates larger values for the RF method.

with values obtained with RF methods systematically larger than those obtained with the MRK method.

IV. DISCUSSION

The aim of this study was to provide an overview of emerging radar-based techniques for gait parameter estimation, the results of a pilot study in which we compared the accuracy of different radar-based QGA techniques, and a discussion to highlight areas requiring future research.

Depending on the available technology, gait variables associated with fall risk can range from very simple to complex. Most radar-based gait parameters estimation studies focused on estimating gait speed [55], [56], [61], [64], [102]. Perhaps, gait speed is the most common and simple outcome sensitive to pathology and can be considered as the final common expression of locomotor control [103], with higher risk for falls associated with slower self-selected walking speed. However, gait speed cannot reveal the underlying impairments and measurement of spatio-temporal and biomechanical parameters of gait are useful to augment diagnostic capabilities. The gait pattern in older people at higher risk for falls is usually stiffer, less coordinated, and characterized by poorer postural control, shorter stride length and height, wider step width, and greater propensity of landing flatfoot.

After gait speed, step time is the spatio-temporal parameter that most radar-based studies tried to estimate. The results from this study and other studies show that excellent agreement in average step time recognition is achieved between RF and the Vicon systems [55], independently by the RF processing technique. To the best of our knowledge, few radar-based studies have attempted to validate step length estimation [55], [61]. However, both estimated step length by multiplying step time by the average walking [61] or treadmill [64] speed. Both studies reported small estimation errors of about 2-3%. Instead, we proposed to estimate step length by directly calculating the distance between ankle markers when reconstructing the skeleton or integrating the approximated trunk velocity curve over a step when using the μD. When attempting to estimate spatial components of gait, we observed an underestimation of the average step length of about 13% when using the μD method. Using either of the RF skeleton methods significantly improved the estimation performance. Using SkelR, we obtained an overestimation of only 2% of step length. When using SkelS, estimation can be further improved to 1% of error. It should be taken into account that estimating spatiotemporal parameters using body point locations allow researchers to estimate a large number of spatio-temporal parameters such as step width, joint angles, and others.

Although the significant differences in the gait pattern of fallers and non-fallers, few quantitative studies have found measures of gait that can predict fall risk. A promising method to assess fall risk is the evaluation of gait stability parameters derived from biomechanics and dynamical systems theories [104], [105], [106], [107]. Briefly, repetitive motor tasks, like walking, can be treated as a nonlinear dynamic system where variables have a cyclic behavior and recur iteratively with almost the same pattern during the temporal evolution of the task. This pseudo-periodic behavior can be exploited to quantify gait variability and nonlinear analysis. Alternatively, from a biomechanical point of view, dynamic stability can be defined as a measure of the distance between the center of mass and the base of support [108], [109], [110]. Features describing the variability and complexity of gait are the most sensible in assessing fall risk, as compared with standard quantitative measures of gait [111], [112], [113], [114].

Accurate estimation of gait parameters at each gait cycle is fundamental to estimate gait dynamics. In radar research, this has been attempted in a few studies [55], [56], [61], [64], [115], but they did not systematically analyze gait variability. To the best of our knowledge, our group has been the first to evaluate the performance of RF sensors in estimating gait stability [62], [63], [71]. The pilot study in this work reveals that both micro-Doppler and skeleton estimation-based RF data analysis methods result in measures of variability that show poor to moderate agreement and overestimations of about 100% with respect to the Vicon system. To put this in perspective, it should be noted that previous studies that determined the concurrent validity of gait variability measures obtained with inertial sensors [101], [116], [117], [118], [119] also showed that IMU-based measures have poor to moderate validity [120].

Although the small sample of young participants limited the power of the statistical tests and the generalization of our results to other populations at risk of falling, the pilot study was intended to provide an initial comparison of radar-based techniques for gait analysis and inform the reader about the current limitations of radar technology and the relationship between the specific

radar hardware and accuracy. Even if this preliminary study did not provide real evidence that the system could properly identify signature gait characteristic of faller vs. non faller, the analysis of healthy young adults is the first step in developing a base for further studies on vulnerable populations. Future studies will focus on fall-prone older adults with diagnosed balance problems.

Next, we discuss the limitations of the specific commercially available radar used in the pilot study and aspects of current estimation techniques that adversely affected the accuracy of gait variability measures.

Hardware Limitations: The TI IWR2243 Cascade radar has the advantage of high angular resolution in the azimuth direction due to the ability of exploiting TDM to form a large 192 element virtual array – the more the number of virtual array elements, the finer the angular resolution. However, TDM requires multiple sweeps, which greatly increases the time required to form the virtual array (also known as a coherent processing interval, or CPI) and lowers the overall sample rate. In the pilot study, while the Vicon had a data rate of 100 Hz, the radar was operated at a data rate of just 10 Hz. Our results show that this rate is too low for adequate assessment of gait variability. Furthermore, it should be noted that the TI IWR2243 Cascade radar is able to achieve high angular resolution in just the azimuth direction: with only a few array elements in elevation, the elevation resolution is extremely poor. In depth, the 4 GHz bandwidth of the TI IWR2243 Cascade radar results in 3.75 cm depth resolution. Our results show that the accuracy of estimating skeletal key points is correlated with the radar's resolution; thus, the best accuracy was obtained in estimating position along the azimuth – the direction along which the radar had the highest resolution. Ideally, the optimal radar for gait parameter estimation would have both a low CPI, high bandwidth, and a large number of physical array elements in both the azimuth and elevation. Such a radar, however, results in such a large amount of data from the resulting 4D radar tensor that real-time processing on the edge becomes challenging. To resolve this dilemma in automotive applications, radar design companies have developed RF-system-on-a-chip (RF-SoC) that integrates the RF transceiver circuits with memory blocks, microprocessors and digital signal processing as a complex single-chip system. However, automotive RF-SoCs typically generate real-time point clouds, and do not provide developers access to the raw radar I/Q data required for computation of the micro-Doppler signature or accurate skeleton estimation. Moreover, there is a cost versus performance trade-off in commercially available radar sensors – the larger the antenna arrays and greater the bandwidth, the higher the resolution and performance, but also the greater the cost. Thus, an open research question for gait parameter estimation is whether it would be better to use multiple, low-cost single-channel radars of high bandwidth or a single, more expensive multi-channel, high bandwidth radar.

Processing Constraints: The RF data representation from which gait parameter estimates are derived impacts both accuracy and the parameters that can be estimated. Established metrics for fall risk are based on accurate estimation of skeletal keypoints, which our study also shows offers improved estimation despite hardware limitations. An examination of the RF skeleton estimation literature shows that the more physical variables measured by the radar are used in the estimation process, the greater the accuracy of the resulting estimates. Thus, we have seen an improvement in accuracy when both range, angle, and Doppler are considered relative to range, angle, or micro-Doppler only. Here we should also make a distinction between methods that take as input the radar data tensor (range-frequency-angle vs. time) versus methods that directly use radar point clouds. While the use of point clouds may seem expedient given its ready availability from commercially available RF-SoCs, the point cloud is itself a derived data representation based on the constant false-alarm rate (CFAR) detection applied to the radar data tensor. Although more recently developed RF-SoCs provide not just (x, y, z) coordinates for each point but also a Doppler shift (f_D) measurement, it should be noted that these measurements are provided every CPI, which is the duration that N pulses can be transmitted at a pulse repetition interval (PRI) for each pulse. In contrast, a micro-Doppler signature contains a Fast Fourier Transform (FFT)-based estimate of micro-Doppler frequency (radial velocity) at an interval of PRI/N_{fft}, where N_{fft} is the number of FFT points utilized. As such, the micro-Doppler represents a much richer source of kinematic information than that embodied by point clouds. Thus, an open area of research is how to best process the RF data tensor to maximally exploit the complete set of measurements by a radar system for gait parameter estimation – and how to accomplish this in real-time to minimize latency and maximize sample rate.

DNN Design Considerations: The most widely used DNNs are networks that were proposed for the applications of computer vision and speech processing. However, radar data is not inherently an image, nor does it possess the same frequency-dependent properties as speech signals [121]. Consequently, from a DNN design perspective as well the RF data representation utilized at the input of a DNN will have a great impact on the resulting performance [122] both in terms of accuracy and latency. For example, direct utilization of the complex I/Q radar data at the input of a CNN can reduce computation time, enabling real-time applications, but has greatly degraded performance relative to that of utilization of the micro-Doppler signature at the input. Recently, the inclusion of complex sinc filtering layers prior to the convolutional layers has been proposed to attain comparable performance with low latency [123]. Another disadvantage of CNN-based skeleton estimation methods is that they do not consider the spatial correlation inherent to human movement. Although the CNN+LSTM model does incorporate sample-to-sample correlations, our pilot study examining results on simulated data is evidence that there remains a significant amount of estimation uncertainty due to network design and training. Finally, it should be noted that deep learning-based methods are very data greedy, and that not just the amount of data but also how the data was collected – under what scenarios, sensor positions, environment, and the mobility characteristics of the participants utilized – will impact model training and resulting estimation accuracy. Thus, there remains much

opportunity for future research in DNN design that can contribute to improved radar-based gait parameter estimation accuracy.

Environmental Factors: In application of radar-based QGA technologies in home, signal processing and AI/ML algorithms must also take into consideration dynamic environmental factors, such as the separation of radar signatures from multiple people [124], [125], [126] and potential presence of obstacles or other sources of motion in the scene being illuminated by the radar, such as a fan or pet. Thus, while on the one hand researchers are developing more advanced signal processing and micro-Doppler decomposition [127], [128], [129] algorithms, on the other hand some researchers have proposed positioning the radar in hallways [56], where obstacles are not expected and motion is automatically constrained by the walls, or utilizing the radar in a cognizant fashion by potential users, such as the case would be if conducting an in-home TUG test. Dynamic environmental factors, including sensor positioning, will also impact the ability of DNNs to generalize across environments and thus must be accounted for during training and network design.

V. Conclusion

This paper has provided an overview of emerging radar-based techniques for gait parameter estimation, especially with emphasis on those relevant to fall risk. A pilot study was conducted that compares the accuracy of gait parameters estimation from different radar data representations (i.e., micro-Doppler signature and skeletal point estimates) against an 8-camera, marker-based optical tracking system. The results of this study show that while there is excellent agreement between radar and optical tracking estimates of step time and step length, gait variability measures show poor to moderate agreement. The limitations of current radar-based technology that adversely affect the accuracy of radar-based gait variability measures – such as trade-offs between transceiver architecture, transmit waveform parameters, and cost, processing constraints, and DNN design considerations – are discussed. We conclude by pointing out areas for future research that can address current limitations and enable the realization of radar-based QGA as a promising emerging technology for continuous, non-intrusive fall risk assessment.

Conflict of Interest

The authors declare that they have no commercial or financial relationships that could be construed as a potential conflict of interest.

Author Contribution

S.Z. Gurbuz, M.M. Rahman, and D. Martelli contributed to the conception and design of the study, algorithm development, interpretation of results and manuscript writing. Z. Bassiri contributed to the data collection and curation. S. Z. Gurbuz and M. M. Rahman were primarily responsible for the radar-related sections of the paper, while D. Martelli focused on biomechanics, gait analysis and pilot study sections of the paper. Additionally, each author contributed their specialized expertise in their respective research domains to the overall interpretation, discussions and insights offered by the paper, as well as reviewing and editing the manuscript.

Acknowledgment

This study was conducted with approval of the University of Alabama Institutional Review Board (IRB) under Protocols #18-06-1271, #21-10-5055, and #23-04-6553.

References

[1] L. Z. Rubenstein, A. S. Robbins, B. L. Schulman, J. Rosado, D. Osterweil, and K. R. Josephson, "Falls and instability in the elderly," *J. Amer. Geriatrics Soc.*, vol. 36, pp. 266–278, 1988.
[2] T. Masud and R. O. Morris, "Epidemiology of falls," *Age Ageing*, vol. 30, no. Suppl 4, pp. 3–7, 2001.
[3] W. P. Berg, H. M. Alessio, E. M. Mills, and C. Tong, "Circumstances and consequences of falls in independent community-dwelling older adults," *Age Ageing*, vol. 26, no. 4, pp. 261–268, 1997.
[4] T. E. Lockhart, "An integrated approach towards identifying age-related mechanisms of slip initiated falls," *J. Electromyogr. Kinesiol.*, vol. 18, no. 2, pp. 205–217, 2008.
[5] S. N. Robinovitch et al., "Video capture of the circumstances of falls in elderly people residing in long-term care: An observational study," *Lancet*, vol. 381, no. 9860, pp. 47–54, 2013.
[6] A. F. Ambrose, G. Paul, and J. M. Hausdorff, "Risk factors for falls among older adults: A review of the literature," *Maturitas*, vol. 75, no. 1, pp. 51–61, 2013.
[7] M. Job, A. Dottor, A. Viceconti, and M. Testa, "Ecological gait as a fall indicator in older adults: A systematic review," *Gerontologist*, vol. 60, no. 5, pp. e395–e412, 2020.
[8] A. H. Snijders, B. P. van de Warrenburg, N. Giladi, and B. R. Bloem, "Neurological gait disorders in elderly people: Clinical approach and classification," *Lancet Neurol.*, vol. 6, no. 1, pp. 63–74, 2007.
[9] G. Allali, E. I. Ayers, R. Holtzer, and J. Verghese, "The role of postural instability/gait difficulty and fear of falling in predicting falls in non-demented older adults," *Arch. Gerontol. Geriatrics*, vol. 69, pp. 15–20, 2017.
[10] M. Montero-Odasso, J. Verghese, O. Beauchet, and J.M. Hausdorff, "Gait and cognition: A complementary approach to understanding brain function and the risk of falling," *J. Amer. Geriatrics Soc.*, vol. 60, no. 11, pp. 2127–2136, 2012.
[11] J.G. Nutt, F. B. Horak, and B. R. Bloem, "Milestones in gait, balance, and falling," *Movement Disord.*, vol. 26, no. 6, pp. 1166–1174, 2011.
[12] D. Hamacher, N. B. Singh, J. H. Van Dieen, M. O. Heller, and W.R. Taylor, "Kinematic measures for assessing gait stability in elderly individuals: A systematic review," *J. Roy. Soc. Interface*, vol. 8, no. 65, pp. 1682–1698, 2011.
[13] Y. Zhang, M. Wang, J. Awrejcewicz, G. Fekete, F. Ren, and Y. Gu, "Using gold-standard gait analysis methods to assess experience effects on lower-limb mechanics during moderate high-heeled jogging and running," *J. Vis. Exp.*, vol. 14, no. 127, Sep. 2017, Art. no. 55714.
[14] J. Jeon et al., "Influence of the Hawthorne effect on spatiotemporal parameters, kinematics, ground reaction force, and the symmetry of the dominant and nondominant lower limbs during gait," *J. Biomech.*, vol. 152, 2023, Art. no. 111555.
[15] C. Malchow and G. Fiedler, "Effect of observation on lower limb prosthesis gait biomechanics: Preliminary results," *Prosthetics Orthotics Int.*, vol. 40, pp. 739–743, 2016.
[16] V.-R. Xefteris, A. Tsanousa, G. Meditskos, S. Vrochidis, and I. Kompatsiaris, "Performance, challenges, and limitations in multimodal fall detection systems: A review," *IEEE Sensors J.*, vol. 21, no. 17, pp. 18398–18409, Sep. 2021.
[17] M. G. Amin, Y. D. Zhang, F. Ahmad, and K. C. D. Ho, "Radar signal processing for elderly fall detection: The future for in-home monitoring," *IEEE Signal Process. Mag.*, vol. 33, no. 2, pp. 71–80, Mar. 2016.
[18] S. Z. Gurbuz and M. G. Amin, "Radar-based human-motion recognition with deep learning: Promising applications for indoor monitoring," *IEEE Signal Process. Mag.*, vol. 36, no. 4, pp. 16–28, Jul. 2019.

[19] B. Y. Su, K. C. Ho, M. J. Rantz, and M. Skubic, "Doppler radar fall activity detection using the wavelet transform," *IEEE Trans. Biomed. Eng.*, vol. 62, no. 3, pp. 865–875, Mar. 2015.

[20] C. Garripoli et al., "Embedded DSP-based telehealth radar system for remote in-door fall detection," *IEEE J. Biomed. Health Inform.*, vol. 19, no. 1, pp. 92–101, Jan. 2015.

[21] B. Jokanović and M. Amin, "Fall detection using deep learning in range-Doppler radars," *IEEE Trans. Aerosp. Electron. Syst.*, vol. 54, no. 1, pp. 180–189, Feb. 2018.

[22] E. Cippitelli, F. Fioranelli, E. Gambi, and S. Spinsante, "Radar and RGB-depth sensors for fall detection: A review," *IEEE Sensors J.*, vol. 17, no. 12, pp. 3585–3604, Jun. 2017.

[23] F. Fioranelli, J. Le Kernec, and S. A. Shah, "Radar for health care: Recognizing human activities and monitoring vital signs," *IEEE Potentials*, vol. 38, no. 4, pp. 16–23, Jul./Aug. 2019.

[24] B. Çağlıyan and S. Z. Gürbüz, "Micro-Doppler-based human activity classification using the mote-scale bumblebee radar," *IEEE Geosci. Remote Sens. Lett.*, vol. 12, no. 10, pp. 2135–2139, Oct. 2015.

[25] Y. Kim and T. Moon, "Human detection and activity classification based on micro-Doppler signatures using deep convolutional neural networks," *IEEE Geosci. Remote Sens. Lett.*, vol. 13, no. 1, pp. 8–12, Jan. 2016.

[26] D. P. Fairchild and R. M. Narayanan, "Multistatic micro-Doppler radar for determining target orientation and activity classification," *IEEE Trans. Aerosp. Electron. Syst.*, vol. 52, no. 1, pp. 512–521, Feb. 2016.

[27] K. Saho, M. Fujimoto, M. Masugi, and L.-S. Chou, "Gait classification of young adults, elderly non-fallers, and elderly fallers using micro-Doppler radar signals: Simulation study," *IEEE Sensors J.*, vol. 17, no. 8, pp. 2320–2321, Apr. 2017.

[28] B. Erol and M. G. Amin, "Radar data cube processing for human activity recognition using multisubspace learning," *IEEE Trans. Aerosp. Electron. Syst.*, vol. 55, no. 6, pp. 3617–3628, Dec. 2019.

[29] I. Ullmann, R. G. Guendel, N. C. Kruse, F. Fioranelli, and A. Yarovoy, "A survey on radar-based continuous human activity recognition," *IEEE J. Microw.*, vol. 3, no. 3, pp. 938–950, Jul. 2023.

[30] H. Li, A. Mehul, J. Le Kernec, S. Z. Gurbuz, and F. Fioranelli, "Sequential human gait classification with distributed radar sensor fusion," *IEEE Sensors J.*, vol. 21, no. 6, pp. 7590–7603, Mar. 2021.

[31] Y. Kim, I. Alnujaim, and D. Oh, "Human activity classification based on point clouds measured by millimeter wave MIMO radar with deep recurrent neural networks," *IEEE Sensors J.*, vol. 21, .no. 12, pp. 13522–13529, Jun. 2021.

[32] W. Ding, X. Guo, and G. Wang, "Radar-based human activity recognition using hybrid neural network model with multidomain fusion," *IEEE Trans. Aerosp. Electron. Syst.*, vol. 57, no. 5, pp. 2889–2898, Oct. 2021.

[33] S. Waqar, M. Muaaz, and M. Pätzold, "Direction-independent human activity recognition using a distributed MIMO radar system and deep learning," *IEEE Sensors J.*, vol. 23, no. 20, pp. 24916–24929, Oct. 2023.

[34] M. M. Rahman, S. Z. Gurbuz, and M. G. Amin, "Physics-aware generative adversarial networks for radar-based human activity recognition," *IEEE Trans. Aerosp. Electron. Syst.*, vol. 59, no. 3, pp. 2994–3008, Jun. 2023.

[35] S. Z. Gurbuz, C. Clemente, A. Balleri, and J. J. Soraghan, "Micro-Doppler-based in-home aided and unaided walking recognition with multiple radar and sonar systems," *IET Radar Sonar Navigation*, vol. 11, pp. 107–115, 2017.

[36] M. S. Seyfioğlu, A. M. Özbayoğlu, and S. Z. Gürbüz, "Deep convolutional autoencoder for radar-based classification of similar aided and unaided human activities," *IEEE Trans. Aerosp. Electron. Syst.*, vol. 54, no. 4, pp. 1709–1723, Aug. 2018.

[37] A.-K. Seifert, A. M. Zoubir, and M. G. Amin, "Radar-based human gait recognition in cane-assisted walks," in *Proc. IEEE Radar Conf.*, 2017, pp. 1428–1433.

[38] H. Okinaka et al., "Gait classification of healthy young and elderly adults using micro-Doppler radar remote sensing," in *Proc. IEEE Joint 10th Int. Conf. Soft Comput. Intell. Syst., 19th Int. Symp. Adv. Intell. Syst.*, 2018, pp. 1222–1226.

[39] A.-K. Seifert, A. M. Zoubir, and M. G. Amin, "Radar classification of human gait abnormality based on sum-of-harmonics analysis," in *Proc. IEEE Radar Conf.*, 2018, pp. 0940–0945.

[40] A.-K. Seifert, M. G. Amin, and A. M. Zoubir, "Toward unobtrusive in-home gait analysis based on radar micro-Doppler signatures," *IEEE Trans. Biomed. Eng.*, vol. 66, no. 9, pp. 2629–2640, Sep. 2019.

[41] F. Cai, A. Patharkar, T. Wu, F. Y. M. Lure, H. Chen, and V. C. Chen, "STRIDE: Systematic radar intelligence analysis for ADRD risk evaluation with gait signature simulation and deep learning," *IEEE Sensors J.*, vol. 23, no. 10, pp. 10998–11006, May 2023.

[42] M. A. Richards, *Fundamentals of Radar Signal Processing*, 2nd ed. New York, NY, USA, McGraw Hill, 2014.

[43] V. C. Chen, *The Micro-Doppler Effect in Radar*, 2nd ed. Boston, MA, USA, Artech House, 2019.

[44] S. Z. Gurbuz, S. Sun, and D. Tahmoush, "Radar signals, systems, and phenomenology," in *Deep Neural Network Design for Radar Applications*, S. Z. Gurbuz, Ed. London, U.K.: IET/SciTech Publishing, 2020, pp. 11–36.

[45] R. Schmidt, "Multiple emitter location and signal parameter estimation," *IEEE Trans. Antennas Propag.*, vol. 34, no. 3, pp. 276–280, Mar. 1986.

[46] F. Belfiori, W. van Rossum, and P. Hoogeboom, "Application of 2D MUSIC algorithm to range-azimuth FMCW radar data," in *Proc. IEEE 9th Eur. Radar Conf.*, 2012, pp. 242–245.

[47] J. Li and P. Stoica, *MIMO Radar Signal Processing*. Hoboken, NJ, USA: Wiley, 2009.

[48] J. L. Geisheimer, W.S. Marshall, and E. Greneker, "A continuous-wave (CW) radar for gait analysis," *Signals, Syst., Comput.*, vol. 1, pp. 834–838, 2001.

[49] M. Otero, "Application of a continuous wave radar for human gait recognition," *Proc. SPIE*, vol. 5809, pp. 538–548, 2005.

[50] J. L. Geisheimer, E. F. Greneker, and W. S. Marshall, "A high-resolution Doppler model of human gait," *Radar Sensor Technol. Data Visualization*, SPIE, vol. 4744, Jul. 2002. [Online]. Available: https://www.spiedigitallibrary.org/conference-proceedings-of-spie/4744/1/High-resolution-Doppler-model-of-the-human-gait/10.1117/12.488286.short

[51] P. van Dorp and F.C.A. Groen, "Human walking estimation with radar," *IEE Proc. Radar, Sonar Navigation*, vol. 150, no. 5, pp. 356–365, Oct. 2003.

[52] R. Boulic, M. N. Thalmann, and D. Thalmann, "A global human walking model with real-time kinematic personification," *Vis. Comput.*, vol. 6, pp. 344–358, 1990.

[53] S. Z. Gurbuz, W. L. Melvin, and D. B. Williams, "Detection and identification of human targets in radar," *Proc. SPIE*, vol. 6567, pp. 185–195, 2007.

[54] S. Z. Gurbuz, W. L. Melvin, and D. B. Williams, "Kinematic model-based human detectors for multi-channel radar," *IEEE Trans. Aerosp. Electron. Syst.*, vol. 48, no. 2, pp. 1306–1318, Apr. 2012.

[55] F. Wang, M. Skubic, M. Rantz, and P. E. Cuddihy, "Quantitative gait measurement with pulse-Doppler radar for passive in-home gait assessment," *IEEE Trans. Biomed. Eng.*, vol. 61, no. 9, pp. 2434–2443, Sep. 2014.

[56] H. Abedi, J. Boger, P. P. Morita, A. Wong, and G. Shaker, "Hallway gait monitoring using novel radar signal processing and unsupervised learning," *IEEE Sensors J.*, vol. 22, no. 15, pp. 15133–15145, Aug. 2022.

[57] D. Alshamaa, R. Soubra, and A. Chkeir, "A radar sensor for automatic gait speed analysis in walking tests," *IEEE Sensors J.*, vol. 21, no. 12, pp. 13886–13894, Jun. 2021.

[58] F. Quaiyum, N. Tran, J. E. Piou, O. Kilic, and A. E. Fathy, "Noncontact human gait analysis and limb joint tracking using Doppler radar," *IEEE J. Electromagnetics, RF Microw. Med. Biol.*, vol. 3, no. 1, pp. 61–70, Mar. 2019.

[59] F. Foroughian et al., "Non-contact multi-subject human gait analysis using a state-space method with enhanced 1-D block representation," *IEEE J. Electromagnetics, RF Microw. Med. Biol.*, vol. 5, no. 2, pp. 155–167, Jun. 2021.

[60] S. P. Rana, M. Dey, M. Ghavami, and S. Dudley, "Non-contact human gait identification through IR-UWB edge-based monitoring sensor," *IEEE Sensors J.*, vol. 19, no. 20, pp. 9282–9293, Oct. 2019.

[61] K. Saho, K. Shioiri, S. Kudo, and M. Fujimoto, "Estimation of gait parameters from trunk movement measured by Doppler radar," *IEEE J. Electromagnetics, RF Microw. Med. Biol.*, vol. 6, no. 4, pp. 461–469, Dec. 2022.

[62] M. M. Rahman, D. Martelli, and S. Z. Gurbuz, "Gait variability analysis with multi-channel FMCW radar for fall risk assessment," in *Proc. IEEE 12th Sensor Array Multichannel Signal Process. Workshop*, 2022, pp. 345–349.

[63] S. Z. Gurbuz, M. M. Rahman, E. Kurtoglu, and D. Martelli, "Continuous human activity recognition and step-time variability analysis with FMCW radar," in *Proc. IEEE-EMBS Int. Conf. Biomed. Health Inform.*, 2022, pp. 1–4.

[64] A.-K. Seifert, M. Grimmer, and A. M. Zoubir, "Doppler radar for the extraction of biomechanical parameters in gait analysis," *IEEE J. Biomed. Health Inform.*, vol. 25, no. 2, pp. 547–558, Feb. 2021.

[65] K. Saho, M. Fujimoto, M. Masugi, and L.-S. Chou, "Gait classification of young adults, elderly non-fallers, and elderly fallers using micro-Doppler radar signals: Simulation study," *IEEE Sensors J.*, vol. 17, no. 8, pp. 2320–2321, Apr. 2017.

[66] K. Saho, K. Shioiri, M. Fujimoto, and Y. Kobayashi, "Micro-Doppler radar gait measurement to detect age- and fall risk-related differences in gait: A simulation study on comparison of deep learning and gait parameter-based approaches," *IEEE Access*, vol. 9, pp. 18518–18526, 2021.

[67] K. Saho, M. Fujimoto, Y. Kobayashi, and M. Matsumoto, "Experimental verification of micro-Doppler radar measurements of fall-risk-related gait differences for community-dwelling elderly adults," *Sensors*, vol. 22, no. 3, Jan. 2022, Art. no. 930.

[68] K. Shioiri, K. Saho, M. Fujimoto, and Y. Kobayashi, "Radar-based gait classification of elderly non-fallers and multiple fallers using machine learning," in *Proc. IEEE 3rd Glob. Conf. Life Sci. Technol.*, 2021, pp. 399–400.

[69] K. Saho, K. Uemura, K. Sugano, and M. Matsumoto, "Using micro-Doppler radar to measure gait features associated with cognitive functions in elderly adults," *IEEE Access*, vol. 7, pp. 24122–24131, 2019.

[70] J. C. Ayena, L. Chioukh, M.J.-D. Otis, and D. Deslandes, "Risk of falling in a timed up and go test using an UWB radar and an instrumented insole," *Sensors*, vol. 21, no. 3, 2021, Art. no. 722.

[71] A. Ntanis, N. Kostikis, I. Tsimperis, K. Tsiouris, G. Rigas, and D. Fotiadis, "Evaluating parameters of the TUG test based on data from IMU and UWB sensors," in *Proc. IEEE 18th Int. Conf. Wireless Mobile Comput., Netw. Commun.*, 2022, pp. 142–147.

[72] R. Soubra, R. Mourad-Chehade, and A. Chkeir, "Automation of the timed up and go test using a Doppler radar system for gait and balance analysis in elderly people," *J. Healthcare Eng.*, vol. 2023, 2023, Art. no. 2016262.

[73] B. Erol and M. G. Amin, "Radar data cube processing for human activity recognition using multisubspace learning," *IEEE Trans. Aerosp. Electron. Syst.*, vol. 55, no. 6, pp. 3617–3628, Dec. 2019.

[74] B. Erol and M. G. Amin, "Radar data cube analysis for fall detection," in *Proc. IEEE Int. Conf. Acoust., Speech Signal Process.*, 2018, pp. 2446–2450.

[75] S. Z. Gurbuz, E. Kurtoglu, M. M. Rahman, and D. Martelli, "Gait variability analysis using continuous RF data streams of human activity," *Smart Health*, vol. 26, 2022, Art. no. 100334.

[76] Y. Liu et al., "Monitoring gait at home with radio waves in parkinson's disease: A marker of severity, progression, and medication response," *Sci. Transl. Med.*, vol. 14, 2022, Art. no. eadc9669.

[77] C.-Y. Hsu, Y. Liu, Z. Kabelac, R. Hristov, D. Katabi, and C. Liu, "Extracting gait velocity and stride length from surrounding radio signals," in *Proc. CHI Conf. Hum. Factors Comput. Syst.*, 2017, pp. 2116–2126.

[78] D. Wang, J. Park, H.-J. Kim, K. Lee, and S. H. Cho, "Noncontact extraction of biomechanical parameters in gait analysis using a multi-input and multi-output radar sensor," *IEEE Access*, vol. 9, pp. 138496–138508, 2021.

[79] T. Mao, Y Zhang, K. Zhu, T. Wang, and H. Sun, "Estimation of human gait features by trajectory tracking and recombination using radar range-Doppler-time data," *IET Radar, Sonar, Navigation*, vol. 17, no. 2, pp. 236–246, 2023.

[80] F. Adib, C.-Y. Hsu, H. Mao, D. Katabi, and F. Durand, "Capturing the human figure through a wall," *ACM Trans. Graph.*, vol. 34, no. 6, pp. 1–13, 2015.

[81] M. Zhao et.al., "Rf-based 3D skeletons," in *Proc. Conf. ACM Special Int. Group Data Commun.*, 2018, pp. 267–281.

[82] A. Sengupta, F. Jin, R. Zhang, and S. Cao, "mm-Pose: Real-time human skeletal posture estimation using mmWave radars and CNNs," *IEEE Sensors J.*, vol. 20, no. 17, pp. 10 032–10 044, Sep. 2020.

[83] S. Hu, A. Sengupta, and S. Cao, "Stabilizing skeletal pose estimation using mmwave radar via dynamic model and filtering," in *Proc. IEEE Int. Conf. Biomed. Health Inform.*, 2022, pp. 1–6.

[84] S. An and U. Y. Ogras, "Mars: mmWave-based assistive rehabilitation system for smart healthcare," *ACM Trans. Embedded Comput. Syst.*, vol. 20, no. 5s, pp. 1–22, 2021.

[85] S. P. Lee, "HuPR: A benchmark for human pose estimation using millimeter wave radar," in *Proc. IEEE/CVF Winter Conf. Appl. Comput. Vis.*, 2023, pp. 5704–5713.

[86] H. Xue et al., "Towards generalized mmWave-based human pose estimation through signal augmentation," in *Proc. 29th Annu. Int. Conf. Mobile Comput. Netw.*, 2023, pp. 1–15.

[87] H. Xue et al., "M4esh: mmWave-based 3D human mesh construction for multiple subjects," in *Proc. 20th ACM Conf. Embedded Networked Sensor Syst.*, 2022, pp. 391–406.

[88] S. Hu, S. Cao, N. Toosizadeh, J. Barton, M. G. Hector, and M. J. Fain, "mmPose-FK: A forward kinematics approach to dynamic skeletal pose estimation using mmWave radars," *IEEE Sensors J.*, vol. 24, no. 5, pp. 6469–6481, Mar. 2024.

[89] Z. Cao, W. Ding, R. Chen, J. Zhang, X. Guo, and G. Wang, "A joint global–local network for human pose estimation with millimeter wave radar," *IEEE Internet Things J.*, vol. 10, no. 1, pp. 434–446, Jan. 2023.

[90] C. Xie, D. Zhang, Z. Wu, C. Yu, Y. Hu, and Y. Chen, "RPM 2.0: RF-based pose machines for multi-person 3D pose estimation," *IEEE Trans. Circuits Syst. Video Technol.*, vol. 34, no. 1, pp. 490–503, Jan. 2024.

[91] C. Xie, D. Zhang, Z. Wu, C. Yu, Y. Hu, and Y. Chen, "RPM: RF-based pose machines," *IEEE Trans. Multimedia*, vol. 26, pp. 637–649, 2024.

[92] X. Zhou, T. Jin, Y. Dai, Y. Song, and Z. Qiu, "MD-pose: Human pose estimation for single-channel UWB radar," *IEEE Trans. Biometrics, Behav., Identity Sci.*, vol. 5, no. 4, pp. 449–463, Oct. 2023.

[93] M. M. Rahman, D. Martelli, and S. Z. Gurbuz, "Radar-based human skeleton estimation with CNN-LSTM network trained with limited data," in *Proc. IEEE EMBS Int. Conf. Biomed. Health Inform.*, 2023, pp. 1–4.

[94] Q. Wang, G. Kurillo, F. Ofli, and R. Bajcsy, "Evaluation of pose tracking accuracy in the first and second generations of microsoft kinect," in *Proc. IEEE Int. Conf. Healthcare Inform.*, 2015, pp. 380–389.

[95] M. Ota et al., "Verification of reliability and validity of motion analysis systems during bilateral squat using human pose tracking algorithm," *Gait Posture*, vol. 80, pp. 62–67, 2020.

[96] M. S. Seyfioglu, B. Erol, S. Z. Gurbuz, and M. G. Amin, "DNN transfer learning from diversified micro-Doppler for motion classification," *IEEE Trans. Aerosp. Electron. Syst.*, vol. 55, no. 5, pp. 2164–2180, Oct. 2019.

[97] C. Karabacak, S. Z. Gurbuz, A. C. Gurbuz, M. B. Guldogan, G. Hendeby, and F. Gustafsson, "Knowledge exploitation for human micro-Doppler classification," *IEEE Geosci. Remote Sens. Lett.*, vol. 12, no. 10, pp. 2125–2129, Oct. 2015.

[98] B. Erol, C. Karabacak, and S. Z. Gurbuz, "A kinect-based human micro-Doppler simulator," *IEEE Aerosp. Electron. Syst. Mag.*, vol. 30, no. 5, pp. 6–17, May 2015.

[99] P. J. Huber, "Robust estimation of a location parameter," *Ann. Math. Statist.*, vol. 35, no. 1, pp. 73–101, Mar. 1964.

[100] W. Zijlstra and A. L. Hof, "Assessment of spatio-temporal gait parameters from trunk accelerations during human walking," *Gait Posture*, vol. 18, no. 2, pp. 1–10, 2003.

[101] A. Godfrey, S. Del Din, G. Barry, J. C. Mathers, and L. Rochester, "Instrumenting gait with an accelerometer: A system and algorithm examination," *Med. Eng. Phys.*, vol. 37, no. 4, pp. 400–407, 2015.

[102] P. P. Morita et al., "Comparative analysis of gait speed estimation using wideband and narrowband radars, thermal camera, and motion tracking suit technologies," *J. Healthcare Inform. Res.*, vol. 4, no. 3, pp. 215–237, 2020.

[103] S. Lord, B. Galna, and L. Rochester, "Moving forward on gait measurement: Toward a more refined approach," *Movement Disord.*, vol. 28, no. 11, pp. 1534–1543, 2013.

[104] S. M. Bruijn, O. G. Meijer, P. J. Beek, and J. H. van Dieen, "Assessing the stability of human locomotion: A review of current measures," *J. Roy. Soc. Interface*, vol. 10, no. 83, 2013, Art. no. 20120999.

[105] L. Bizovska, Z. Svoboda, M. Janura, M. C. Bisi, and N. Vuillerme, "Local dynamic stability during gait for predicting falls in elderly people: A one-year prospective study," *PLoS One*, vol. 13, no. 5, 2018, Art. no. e0197091.

[106] E. A. F. Ihlen, A. Weiss, Y. Beck, J. L. Helbostad, and J. M. Hausdorff, "A comparison study of local dynamic stability measures of daily life walking in older adult community-dwelling fallers and non-fallers," *J. Biomech.*, vol. 49, no. 9, pp. 1498–1503, 2016.

[107] T.E. Lockhart and J. Liu, "Differentiating fall-prone and healthy adults using local dynamic stability," *Ergonomics*, vol. 51, no. 12, pp. 1860–1872, 2008.

[108] J. Howcroft, J. Kofman, and E. D. Lemaire, "Review of fall risk assessment in geriatric populations using inertial sensors," *J. Neuroengineering Rehabil.*, vol. 10, no. 1, 2013, Art. no. 91.

[109] S. M. Rispens, K. S. van Schooten, M. Pijnappels, A. Daffertshofer, P. J. Beek, and J. H. van Dieen, "Identification of fall risk predictors in daily

life measurements: Gait characteristics' reliability and association with self-reported fall history," *Neurorehabilitation Neural Repair*, vol. 29, no. 1, pp. 54–61, 2015.

[110] K. S. van Schooten, M. Pijnappels, S. M. Rispens, P. J. Elders, P. Lips, and J. H. van Dieen, "Ambulatory fall-risk assessment: Amount and quality of daily-life gait predict falls in older adults, The journals of gerontology. Series A," *Biol. Sci. Med. Sci.*, vol. 70, no. 5, pp. 608–615, 2015.

[111] M. Job, A. Dottor, A. Viceconti, and M. Testa, "Ecological gait as a fall indicator in older adults: A systematic review," *Gerontologist*, vol. 60, no. 5, pp. e395–e412, Jul. 2020.

[112] M. A. Brodie, Y. Okubo, J. Annegarn, R. Wieching, S. R. Lord, and K. Delbaere, "Disentangling the health benefits of walking from increased exposure to falls in older people using remote gait monitoring and multi-dimensional analysis," *Physiol. Meas.*, vol. 38, pp. 45–62, 2017.

[113] W. D. Kearns et al., "Path tortuosity in everyday movements of elderly persons increases fall prediction beyond knowledge of fall history, medication use, and standardized gait and balance assessments," *J. Amer. Med. Directors Assoc.*, vol. 13, pp. 665.e7–665.e13, 2012.

[114] A. Weiss et al., "Does the evaluation of gait quality during daily life provide insight into fall risk? A novel approach using 3-day accelerometer recordings," *Neurorehabilitation Neural Repair*, vol. 27, no. 8, pp. 742–752, Oct. 2013.

[115] D. Wang, J. Park, H. J. Kim, K. Lee, and S. H. Cho, "Noncontact extraction of biomechanical parameters in gait analysis using a multi-input and multi-output radar sensor," *IEEE Access*, vol. 9, pp. 138496–138508, 2021.

[116] A. Hartmann, S. Luzi, K. Murer, R. A. de Bie, and E. D. de Bruin, "Concurrent validity of a trunk tri-axial accelerometer system for gait analysis in older adults," *Gait Posture*, vol. 29, no. 3, pp. 444–448, 2009.

[117] S. Byun, J. W. Han, T. H. Kim, and K. W. Kim, "Test-retest reliability and concurrent validity of a single tri-axial accelerometer-based gait analysis in older adults with normal cognition," *PLoS One*, vol. 11, no. 7, 2016, Art. no. e0158956.

[118] S. Del Din, A. Godfrey, and L. Rochester, "Validation of an accelerometer to quantify a comprehensive battery of gait characteristics in healthy older adults and Parkinson's disease: Toward clinical and at home use," *IEEE J. Biomed. Health Inform.*, vol. 20, no. 3, pp. 838–847, May 2016.

[119] F. A. Storm, C. J. Buckley, and C. Mazza, "Gait event detection in laboratory and real life settings: Accuracy of ankle and waist sensor based methods," *Gait Posture*, vol. 50, pp. 42–46, 2016.

[120] D. Kobsar et al., "Validity and reliability of wearable inertial sensors in healthy adult walking: A systematic review and meta-analysis," *J. Neuroengineering Rehabil.*, vol. 17, no. 1, 2020, Art. no. 62.

[121] B. Erol, M. G. Amin, and S. Z. Gurbuz, "Automatic data-driven frequency-warped cepstral feature design for micro-Doppler classification," *IEEE Trans. Aerosp. Electron. Syst.*, vol. 54, no. 4, pp. 1724–1738, Aug. 2018.

[122] S. Z. Gurbuz, *Deep Neural Network Design for Radar Applications*. London, U.K.: IET/SciTech Publishing, 2020.

[123] S. Biswas, C. O. Ayna, S. Z. Gurbuz, and A. C. Gurbuz, "CV-SincNet: Learning complex sinc filters from raw radar data for computationally efficient human motion recognition," *IEEE Trans. Radar Syst.*, vol. 1, pp. 493–504, 2023.

[124] X. Huang, J. Ding, D. Liang, and L. Wen, "Multi-person recognition using separated micro-Doppler signatures," *IEEE Sensors J.*, vol. 20, no. 12, pp. 6605–6611, Jun. 2020.

[125] E. Kurtoglu, S. Biswas, A. C. Gurbuz, and S. Z. Gurbuz, "Boosting multi-target recognition performance with MIMO radar-based angular subspace projection and multi-view DNN," *IET Radar Sonar Navigation*, vol. 17, pp. 1115–1128, May 2023.

[126] J. Pegoraro, F. Meneghello, and M. Rossi, "Multiperson continuous tracking and identification from mm-Wave micro-Doppler signatures," *IEEE Trans. Geosci. Remote Sens.*, vol. 59, no. 4, pp. 2994–3009, Apr. 2021.

[127] O. R. Fogle and B. D. Rigling, "Micro-range/micro-Doppler decomposition of human radar signatures," *IEEE Trans. Aerosp. Electron. Syst.*, vol. 48, pp. 3058–3072, Oct. 2012.

[128] W. Li, G. Kuang, and B. Xiong, "Decomposition of multi-component micro-doppler signals based on HHT-AMD," *Appl. Sci.*, vol. 8, 2018, Art. no. 1801.

[129] M. Ostovan, S. Samadi, and A. Kazemi, "DecompNet: Deep Context dependent decomposition network for micro-Doppler signature of walking human," *IEEE Sensors J.*, vol. 21, no. 22, pp. 25862–25869, Nov. 2021.